Vibrational coherences in broadband 2D electronic spectroscopy: spectral filtering vs. excited state displacement.

Dale Green, Giovanni Bressan, Stephen R. Meech and Garth A. Jones

School of Chemistry, University of East Anglia, Norwich, NR4 7TJ, U.K.

e-mail: Dale.Green@uea.ac.uk

Engineering and Physical Sciences Research Council

Introduction

Vibrational coherences in ultrafast 2D electronic spectroscopy (2DES) reveal the motion of nuclear wavepackets, with their intensities governed by the displacement of the electronic excited states with respect to the ground state equilibrium geometry.[1] Recent development of broadband 2DES experiments has enabled access to a greater range of coherences involving higher energy states, providing valuable details of the excited state structure of molecules.[2] Here, combining the equation of motion-phase matching approach for finite laser spectra with the hierarchical equations of motion to correctly account for dephasing and dissipation,[3] we model half-broadband and broadband 2DES of cresyl violet to demonstrate the impact of spectral filtering vs. the relative displacement of two excited states (S_1 and S_n) on the intensity distribution of peaks in the beating maps for two vibrational modes with frequencies 350 cm^{-1} and 585 cm^{-1}.

Open Quantum Systems

The Hamiltonian is split into the system (solute) and the interaction with its environment (solvent).

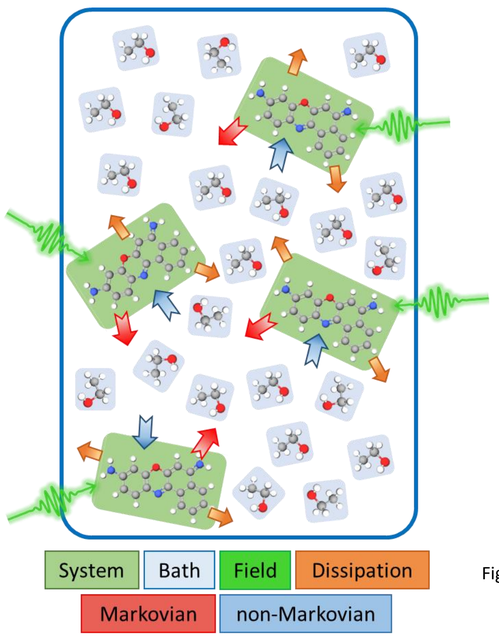

The 585 cm^{-1} and 350 cm^{-1} modes of cresyl violet are modelled as harmonic oscillators coupled to three electronic states, where the excited states S_1 and S_n are displaced along the vibrational coordinate with respect to the minimum of S_0.

Electronic dephasing and vibrational relaxation are then introduced via coupling to the environment, which is approximated as an assembly of harmonic oscillators with coupling strengths determined by the *spectral density*.

Fig 1: Open quantum system. An external laser field excites the system, which then dissipates energy into the bath degrees of freedom, involving both Markovian (system to bath) and non-Markovian (bath to system) information transfer.

Hierarchical Equations of Motion

$$J_n(\omega) = 2\eta_n \frac{\omega\Lambda_n}{\omega^2 + \Lambda_n^2}$$

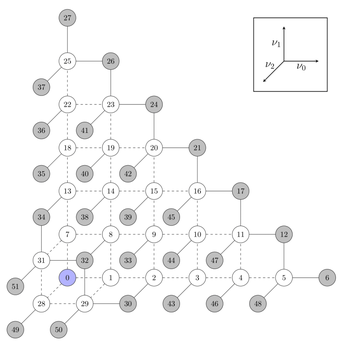

Fig 2: Hierarchy diagram showing connections between ADOs. Each axis is sealed with terminators (grey) and ρ_0 is the reduced density matrix of the system, ρ_S (blue).

Using the Drude spectral density, $J_n(\omega)$, for an overdamped bath, we derive an hierarchy of equations of motion (HEOM).[4] Simultaneous propagation of a series of auxiliary density operators (ADO), $\rho_{\mathbf{j}}(t)$, accounts for non-Markovian memory effects which influence spectral broadening.[5]

$$\dot{\rho}_{\mathbf{j}}(t) = -\left(\frac{i}{\hbar}\mathsf{H}_S^{\times} + \sum_{n=1}^{N}\sum_{k=0}^{M} j_{nk}\nu_{nk}\right)\rho_{\mathbf{j}}(t) - i\sum_{n=1}^{N}\sum_{k=0}^{M} j_{nk}\left(c_{nk}\mathsf{B}_n\rho_{j_{nk}^+}(t) - c_{nk}^*\rho_{j_{nk}^-}(t)\mathsf{B}_n\right)$$
$$-i\sum_{n=1}^{N}\sum_{k=0}^{M}\mathsf{B}_n^{\times}\rho_{j_{nk}^+}(t) - \sum_{n=1}^{N}\left(\frac{2\eta_n}{\hbar\beta\Lambda_n} - \eta_n\cot\left(\frac{\hbar\beta\Lambda_n}{2}\right) - \sum_{k=1}^{M}\frac{c_{nk}}{\nu_{nk}}\right)\mathsf{B}_n^{\times}\mathsf{B}_n^{\times}\rho_{\mathbf{j}}(t)$$

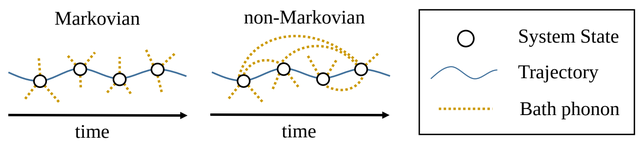

Fig 3: Markovian vs. non-Markovian dynamics. In Markovian, system-bath interactions occur at a constant rate, whilst in non-Markovian, previous interactions can feedback into the system sometime later, requiring a *memory* of previous states, provided by the ADOs.

Termination Criterion

Markovian limit = ξ :

$$\frac{2(M+1)\pi}{\hbar\beta} > \xi \qquad \sum_{n=1}^{N}\sum_{k=0}^{M} j_{nk}\nu_{nk} > \xi$$

2D Electronic Spectroscopy

The interaction of three ultrafast laser pulses, separated by the coherence, τ, and population, T, times, generates a third order polarisation, $P^{(3)}(\tau,T,t)$, in the rephasing and non-rephasing directions.

Spectra are calculated in the impulsive limit from the molecular response function[5] and for finite fields using the equation of motion-phase matching approach (EOM-PMA).[3]

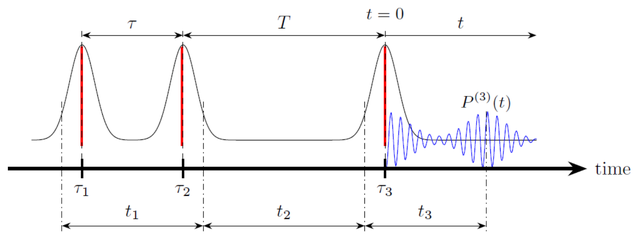

Fig 4: Pulse sequence and waiting times in 2D spectroscopy for impulsive (red) and finite (black) field envelopes.

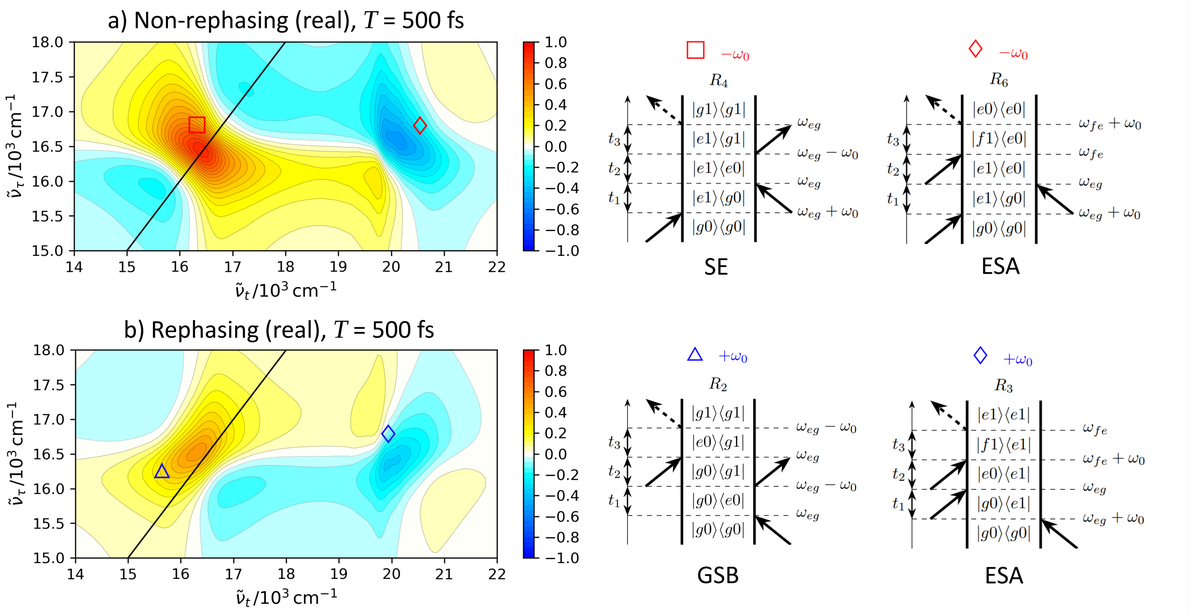

Fig 5: a) Non-rephasing and b) rephasing broadband 2D electronic spectra at T = 500 fs for 585 cm^{-1} cresyl violet vibronic model. The locations of example double-sided Feynman diagrams are shown within the spectra where red (blue) indicates a negative (positive) vibrational coherence and the square, triangle or diamond correspond to stimulated emission (SE), ground state bleach (GSB) or excited state absorption (ESA) pathways, respectively.

Pump-Probe and Femtosecond Coherence Spectra

Pump-probe (PP) spectra are calculated using the same methods as 2DES with $\tau = 0$. Fourier transform of the residuals from a global fit yields the femtosecond coherence spectrum (FCS) at the mode frequency.

With a fixed value of Δ_{10} = 0.63 for the 585 cm^{-1} mode,[6] increasing the displacement between S_1 and S_n expands a vibronic progression in the ESA region, which produces a blueshift in the node of the ESA band in the FCS and significant changes in its intensity relative to the GSB/SE band.

The position of a finite pump spectrum relative to the steady state absorption spectrum also affects the relative intensity of bands in the FCS as well as shifting the node in the GSB/SE band, identifying wavepackets in both the ground and excited electronic states.[7]

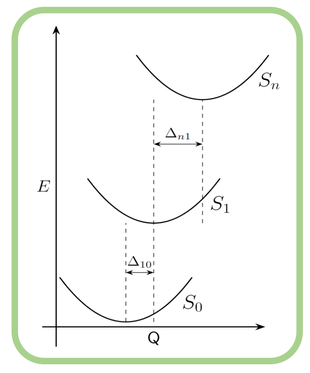

Fig 6: Potential energy surface along the mode coordinate, Q, showing greater displacement between S_1 and S_n than S_0 and S_1.

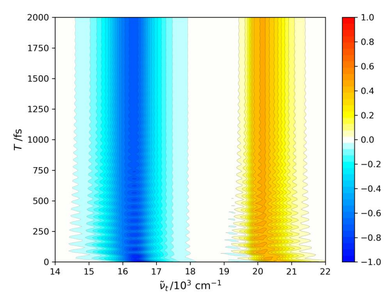

Fig 7: Impulsive PP spectra for 585 cm^{-1} cresyl violet model with Δ_{n1} = 0.6, using opposite convention to 2DES where negative (blue) is GSB/SE and positive (yellow) is ESA.

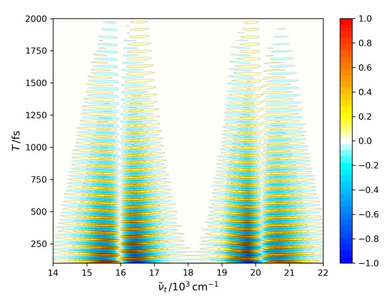

Fig 8: PP residuals for 585 cm^{-1} cresyl violet model with Δ_{n1} = 0.6 after global fit, showing decaying oscillation of excited state wavepacket.

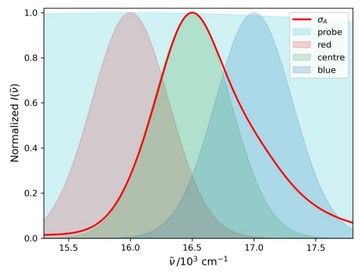

Fig 9: Linear absorption spectrum (red line) for the 585 cm^{-1} mode models with pump (red/centre/blue) and probe spectra used for half-broadband PP and 2DES overlaid.

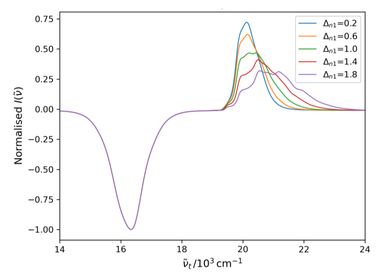

Fig 10: Impulsive PP spectra at T = 2 ps for 585 cm^{-1} cresyl violet models showing a greater vibronic progression in positive ESA band with increasing Δ_{n1}.

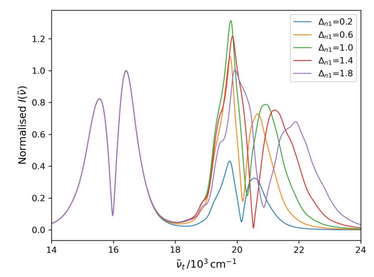

Fig 11: Impulsive FCS for 585 cm^{-1} cresyl violet models showing change in relative intensity of GSB/SE and ESA bands and blueshift of ESA node with increasing Δ_{n1}.

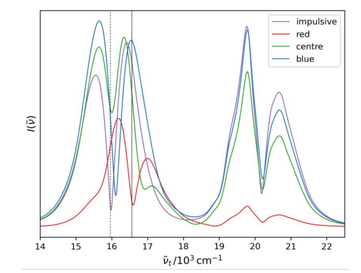

Fig 12: Impulsive FCS for 585 cm^{-1} cresyl violet model with Δ_{n1} = 0.6 compared with FCS using red, centre and blue finite pump spectra. Linear absorption and fluorescence maxima are shown by solid and dashed lines, respectively.

2DES Vibrational Coherence Beating Maps

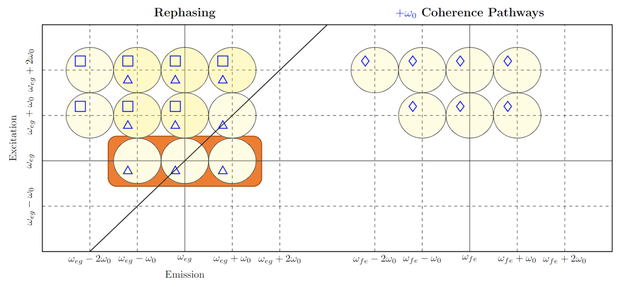

Fig 13: Rephasing positive peak location key diagram with pathways filtered by the finite, blueshifted pump spectrum in fig. 9 highlighted in orange.

Peaks with lower excitation frequency are filtered by a finite, blueshifted pump spectrum in half-broadband beating maps for both the 585 cm^{-1} and 350 cm^{-1} models, whilst the intensity is determined by the relative displacements of the excited states.

The larger displacement between S_1 and S_n for the 350 cm^{-1} model, $\Delta_{n1} \gg \Delta_{10}$, shows the greatest intensity in the ESA region of the beating maps, in contrast to the 585 cm^{-1} model where $\Delta_{n1} \approx \Delta_{10}$ and GSB/SE is most intense.

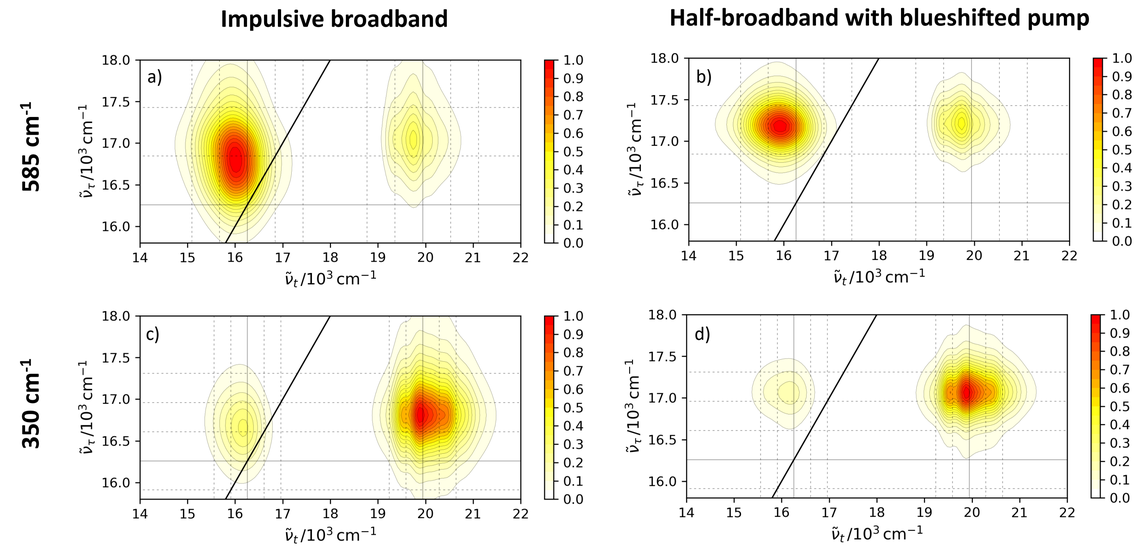

Fig 14: Comparison of the rephasing ω_T = +585 cm^{-1} beating maps for the 585 cm^{-1} cresyl violet model with Δ_{10} = 0.63 and Δ_{n1} = 0.6 calculated (a) in the impulsive limit and (b) with the finite, blueshifted pump spectrum and the rephasing ω_T = +350 cm^{-1} beating maps for the 350 cm^{-1} cresyl violet model with Δ_{10} = 0.18 and Δ_{n1} = 1.4 calculated (c) in the impulsive limit and (d) with the finite, blueshifted pump spectrum.

Conclusion

Separate vibronic models for the 350 cm^{-1} and 585 cm^{-1} modes of cresyl violet demonstrated the filtering of lower excitation frequency peaks in half-broadband 2DES beating maps due to the finite pump spectrum compared with broadband 2DES in the impulsive limit. The relative intensity of the GSB/SE and ESA peaks was also shown to be a result of the relative displacement of the S_1 and S_n excited states with respect to S_0. Future work includes extension to a multimode vibronic model, which introduces new pathways involving both modes, in combination with the new broadband 2DES experiment under development at RAL.

References

1) C.C. Jumper, S. Rafiq, S. Wang, and G.D. Scholes, Curr. Opin. Chem. Biol. **47**, 39 (2018).
2) S. Biswas, J. Kim, X. Zhang, and G.D. Scholes, Chem. Rev. **122**, 4257 (2022).
3) D. Green, F. V. A. Camargo, I.A. Heisler, A.G. Dijkstra, and G.A. Jones, J. Phys. Chem. A **122**, 6206 (2018).
4) Y. Tanimura, J. Chem. Phys. **153**, 020901 (2020).
5) D. Green, B.S. Humphries, A.G. Dijkstra, and G.A. Jones, J. Chem. Phys. **151**, 174112 (2019).
6) G. Batignani, C. Sansone, C. Ferrante, G. Fumero, S. Mukamel, and T. Scopigno, J. Phys. Chem. Lett. **12**, 9239 (2021).
7) G. Bressan, M. Jirasek, P. Roy, H. L. Anderson, S. R. Meech, and I. A. Heisler, Chem. Sci. **13**, 9624 (2022).

Acknowledgements

This study was supported by the Engineering and Physical Sciences Research Council under Awards No. EP/V00817X/1. Calculations presented in this paper were carried out on the High Performance Computing Cluster supported by the Research and Specialist Computing Support service at the University of East Anglia.